Advances in Applied Mathematics and Mechanics
Adv. Appl. Math. Mech., Vol. **7**, No. 2, pp. 135-144

DOI: 10.4208/aamm.2014.m659
April 2015

Total Reflection and Cloaking by Triangular Defects Embedded in Zero Index Metamaterials

Yunqing Huang[1] and Jichun Li[2,*]

[1] *Hunan Key Laboratory for Computation and Simulation in Science and Engineering, Xiangtan University, China*
[2] *Department of Mathematical Sciences, University of Nevada Las Vegas, Las Vegas, Nevada 89154-4020, USA*

Received 12 June 2014; Accepted (in revised version) 26 August 2014

Abstract. In this work, we investigate wave propagation through a zero index metamaterial (ZIM) waveguide embedded with triangular dielectric defects. We provide a theoretical guidance on how to achieve total reflection and total transmission (i.e., cloaking) by adjusting the defect sizes and/or permittivities of the defects. Our work provides a systematical way in manipulating wave propagation through ZIM in addition to the widely studied dielectric defects with cylindrical and rectangular geometries.

AMS subject classifications: 78M10, 65N30, 35L15

Key words: Metamaterials, invisibility cloaks, Maxwell's equatons.

1 Introduction

The past decade saw a growing interest in the study of zero index metamaterials (ZIMs), whose permittivity and permeability are simultaneously or individually near zero. Ziolkowski [1] showed that a matched ZIM slab can be used to transform curved wave fronts into planar ones. Research shows that ZIMs can be used to squeeze electromagnetic (EM) waves [2–4], to perfectly bend and transmit EM waves [5], and to block wave transmission (resulting in total reflection) and conceal objects (cloaking) [6–11]. Such total reflection and total transmission (i.e., cloaking) are realized by embedding proper defects in ZIMs. However, almost all publications on dielectric defects are restricted to cylinderical geometry [8–10].

In this paper, we study the triangular defects case. Three most popular types of triangles are discussed. A systematic guidance for achieving total reflection and cloaking is provided. Extensive full-wave simulations are conducted to verify our analysis. We

*Corresponding author.
Email: huangyq@xtu.edu.cn (Y. Q. Huang), jichun@unlv.nevada.edu (J. C. Li)

 ©2015 Global Science Press

https://doi.org/10.4208/aamm.2014.m659 Published online by Cambridge University Press

like to remark that cloaking realized by embedding proper defects in ZIMs is one of many strategies discussed intensively for cloaking with metamaerials in the past decade (e.g., [15–27] and references cited therein).

2 Realization of total reflection and cloaking

Consider an EM wave incident from the left into a waveguide structure illustrated in Fig. 1. The ZIM region is a metamaterial, whose relative permittivity and permeability are described by the so-called Drude model [6, 12]:

$$\epsilon_1 = \mu_1 = 1 - \frac{\omega_p^2}{\omega(\omega + i\Gamma)},$$

where ω is the excitation angular frequency, ω_p denotes the plasma frequency, and Γ denotes the loss parameter. On both sides of the ZIM region are the free space regions 0 and 3. The defects in region 2, which is embedded in ZIM, are composed of $N \geq 1$ triangles with permittivity and permeability of $\epsilon_{2,k}$ and $\mu_{2,k}$, $k = 1,2,\cdots,N$, respectively. Assuming $\exp(-i\omega t)$ time harmonic factor, the EM wave in each region satisfies the Maxwell's equations: For any $m = 0,1,2,3$,

$$\boldsymbol{H}_m = \frac{1}{i\omega\mu_0\mu_m}\nabla \times \boldsymbol{E}_m, \quad \boldsymbol{E}_m = \frac{i}{\omega\epsilon_0\epsilon_m}\nabla \times \boldsymbol{H}_m. \tag{2.1}$$

Eq. (2.1) can be reduced to the Helmholtz equation:

$$(\partial_{xx} + \partial_{yy} + k_0^2\epsilon_m\mu_m)\boldsymbol{U}_m = 0, \tag{2.2}$$

where $\boldsymbol{U}_m = \boldsymbol{E}_m$ or $\boldsymbol{H}_m$, and $k_0 = \omega\sqrt{\epsilon_0\mu_0}$ is the wave vector in vacuum.

Assume that the walls of the waveguide are made of perfect electric conductor, and the incident wave ($\boldsymbol{H}$ field) propagates to the right along the x direction. By applying Faraday-Maxwell law and Stokes' theorem, we can show that the transmission coefficient

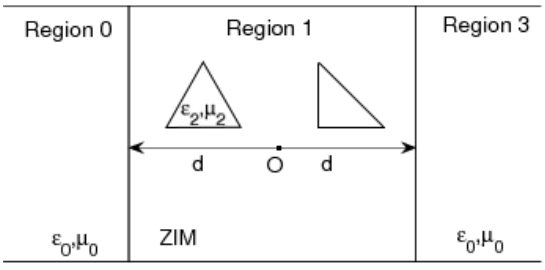


Figure 1: The schematic description of the waveguide structure with vacuum (regions 0 and 3), ZIM (region 1), and embedded triangular defects.

https://doi.org/10.4208/aamm.2014.m659 Published online by Cambridge University Press

is given by (cf. [9,11]):

$$\mathcal{T}=1\Big/\Big[1-\frac{1}{2wH_1}\sum_{k=1}^{N}\oint_{\partial S_{2,k}}\boldsymbol{E}_{2,k}\cdot dl_k\Big], \tag{2.3}$$

where w is the waveguide width, and $\partial S_{2,k}$ denotes the boundary (oriented clockwise) of each defect.

To evaluate $\mathcal{T}$, we need to find the electric field $\boldsymbol{E}_{2,k}$, which can be obtained from Eq. (2.1) once we know the magnetic field $\boldsymbol{H}_{2,k}$ in each defect region. Note that $\boldsymbol{H}_{2,k}$ satisfies Eq. (2.2) with Dirichlet boundary condition $\boldsymbol{H}_{2,k}\cdot\hat{\boldsymbol{t}}=H_1$, where $\hat{\boldsymbol{t}}$ is the unit tangential vector along the boundary of each defect region. Note that it is proved that [11] the boundary data H_1 is constant.

First, we consider an equilateral triangular defect case. For an equilateral triangle $\triangle$ with side length a, permittivity ϵ_2 and permeability μ_2, we can represent the solution $\boldsymbol{H}_{2,k}$ as:

$$\boldsymbol{H}_{2,k}(x,y)=\hat{\boldsymbol{z}}\Big[H_1+\sum_{n,m\geq 1}C_{n,m}\phi_{n,m}(x,y)\Big], \tag{2.4}$$

where $\phi_{n,m}(x,y)$ are the eigenfunctions formed by the symmetric ($\phi^s_{n,m}(x,y)$, $n\geq m$) and anti-symmetric modes ($\phi^a_{n,m}(x,y)$, $n>m$), which are given as [13]:

$$\begin{aligned}
\phi^s_{n,m}(x,y)=&\sin\Big(\frac{\pi l}{3r}(u+2r)\Big)\cos\Big(\frac{\pi(m-n)}{9r}(v-w)\Big)\\
&+\sin\Big(\frac{\pi m}{3r}(u+2r)\Big)\cos\Big(\frac{\pi(n-l)}{9r}(v-w)\Big)\\
&+\sin\Big(\frac{\pi n}{3r}(u+2r)\Big)\cos\Big(\frac{\pi(l-m)}{9r}(v-w)\Big),\\
\phi^a_{n,m}(x,y)=&\sin\Big(\frac{\pi l}{3r}(u+2r)\Big)\sin\Big(\frac{\pi(m-n)}{9r}(v-w)\Big)\\
&+\sin\Big(\frac{\pi m}{3r}(u+2r)\Big)\sin\Big(\frac{\pi(n-l)}{9r}(v-w)\Big)\\
&+\sin\Big(\frac{\pi n}{3r}(u+2r)\Big)\sin\Big(\frac{\pi(l-m)}{9r}(v-w)\Big).
\end{aligned}$$

Here (u,v,w) are the triangular coordinates given by

$$u=r-y,\quad v=\frac{\sqrt{3}}{2}\Big(x-\frac{a}{2}\Big)+\frac{1}{2}(y-r),\quad w=-\frac{\sqrt{3}}{2}\Big(x-\frac{a}{2}\Big)+\frac{1}{2}(y-r),$$

where $r=a/2\sqrt{3}$ is the inradius of the triangle. Note that integers l, m, n satisfy the condition $l+m+n=0$. Due to the orthonormality of $\phi_{n,m}(x,y)$, the coefficient of Eq. (2.4) can be obtained as

$$C_{n,m}=\frac{-k_2^2H_1\int_{\triangle}\phi_{n,m}dxdy}{k_2^2-\lambda_{n,m}}, \tag{2.5}$$

https://doi.org/10.4208/aamm.2014.m659 Published online by Cambridge University Press

where we denote $k_2^2=k_0^2\epsilon_2\mu_2$, and

$$\lambda_{n,m}^2=\frac{2}{27}\left(\frac{\pi}{r}\right)^2(l^2+m^2+n^2)=\frac{4}{27}\left(\frac{\pi}{r}\right)^2(m^2+mn+n^2).$$

Note that the electric field $\boldsymbol{E}_{2,k}$ can be obtained from Eqs. (2.1) and (2.4) as follows:

$$\boldsymbol{E}_{2,k}=\frac{i}{\omega\epsilon_0\epsilon_2}\left[\hat{\boldsymbol{x}}\sum_{n,m\geq 1}C_{n,m}\frac{\partial\phi_{n,m}}{\partial y}-\hat{\boldsymbol{y}}\sum_{n,m\geq 1}C_{n,m}\frac{\partial\phi_{n,m}}{\partial x}\right]. \tag{2.6}$$

By Eqs. (2.3) and (2.6), we see that choosing $k_2^2=\lambda_{n,m}$, i.e.,

$$\epsilon_2=\frac{4}{27}\left(\frac{\pi}{r}\right)^2(m^2+mn+n^2)/(k_0^2\mu_2), \tag{2.7}$$

and $\int_{\triangle}\phi_{n,m}dxdy\neq 0$ makes $C_{n,m}\approx\infty$, which leads to $\mathcal{T}\approx 0$, i.e., in this case total reflection happens.

Using the fact that $\int_{\triangle}\phi_{n,m}dxdy=0$ if and only if $m\neq n$, we see that choosing $m=n$ in Eq. (2.7) leads to total reflection. Otherwise, we will have total transmission, i.e., invisibility cloaking happens.

To justify our analysis, we carried out extensive numerical simulations for various (m,n) modes by using the commercial finite element package COMSOL. For simplicity, we fixed the computational domain $[-0.07,0.07]\text{m}\times[-0.02,0.02]\text{m}$, with the ZIM region $[-0.03,0.03]\text{m}\times[-0.02,0.02]\text{m}$. Moreover, the excitation plane wave has a frequency $f=$ 15GHz, and all defects are assumed to be nonmagnetic (i.e., $\mu_2=1$). All our computations are based on triangular elements with quadratic basis function.

First, we simulate the equilateral triangle defect case. The equilateral triangle has the side length $a=0.02m$. Substituting this into Eq. (2.7) with $k_0=\omega\sqrt{\epsilon_0\mu_0}=2\pi f/c=100\pi$, we obtain

$$\epsilon_2=\frac{4}{27}\left(\frac{1}{100r}\right)^2(m^2+mn+n^2)=\frac{4}{9}(m^2+mn+n^2). \tag{2.8}$$

In Fig. 2, we presented the contour plots of the whole H_z fields obtained with 16576 elements for $m=n=1$ ($\epsilon_2=4\cdot 3/9$), $m=n=2$ ($\epsilon_2=4\cdot 12/9$), and $m=n=3$ ($\epsilon_2=4\cdot 27/9$), respectively. All three cases demonstrate total reflection as expected.

In Fig. 3, we showed three cases for total transmission. The contour plots of the whole H_z fields are obtained with 16576 elements for $m=1$, $n=2$ ($\epsilon_2=4\cdot 7/9$), $m=2$, $n=3$ ($\epsilon_2=4\cdot 19/9$), and $m=1$, $n=5$ ($\epsilon_2=4\cdot 31/9$), respectively.

Now let us consider defect formed by the right isosceles triangle with leg length a, in which case the eigenfunction $\phi_{n,m}$ in Eq. (2.4) is replaced by [14]:

$$\phi_{n,m}(x,y)=\sin\left(\frac{n\pi x}{a}\right)\sin\left(\frac{m\pi y}{a}\right)+(-1)^{n+m+1}\sin\left(\frac{n\pi y}{a}\right)\sin\left(\frac{m\pi x}{a}\right),$$

and the corresponding eigenvalue is $\lambda_{n,m}^2=(n\pi/a)^2+(m\pi/a)^2$.

https://doi.org/10.4208/aamm.2014.m659 Published online by Cambridge University Press

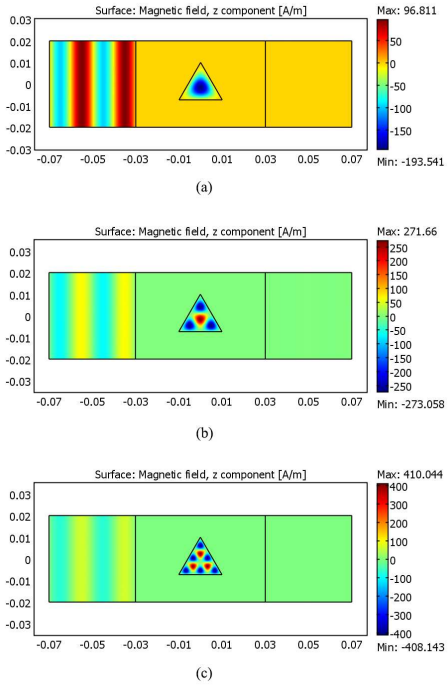


Figure 2: The H_z field for the equilateral triangular defect with $m=n=1$ (a), $m=n=2$ (b), and $m=n=3$ (c).

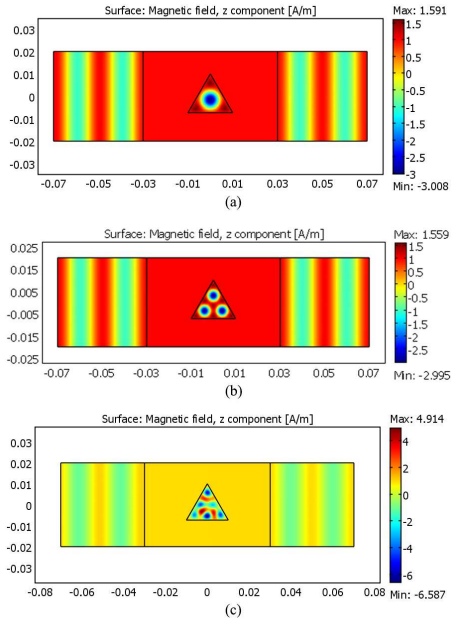


Figure 3: The H_z field for the equilateral triangular defect with $m=1$, $n=2$ (a), $m=2$, $n=3$ (b), and $m=1$, $n=5$ (c).

https://doi.org/10.4208/aamm.2014.m659 Published online by Cambridge University Press

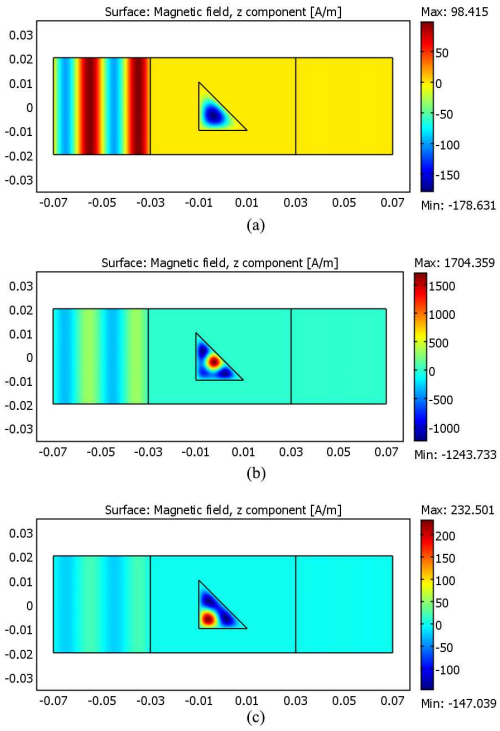


Figure 4: The H_z field for the right isosceles triangular defect with $m=1$, $n=2$ (a), $m=1$, $n=4$ (b), and $m=2$, $n=3$ (c).

Through lengthy derivation, we can show that: If $n=m$ or $n\neq m$, but both are even, then $\int_{\triangle}\phi_{n,m}dxdy=0$; otherwise, we have

$$\int_{\triangle}\phi_{n,m}dxdy=\frac{a}{2m\pi}\left[\frac{2a}{(n+m)\pi}+\frac{2a}{(n+m)\pi}\right]+\frac{2a^2}{mn\pi^2}-\frac{a}{2n\pi}\left[\frac{2a}{(m+n)\pi}+\frac{2a}{(m-n)\pi}\right],$$

using this fact and Eqs. (2.3)-(2.6), we can choose the nonmagnetic defect permittivity as following (assuming the excitation wave frequency $f=15$GHz, and the defect leg length $a=0.02$m): $\epsilon_2=(m^2+n^2)/4$.

In Fig. 4, we demonstrated three total reflection cases obtained with 14848 elements. According to our analysis, the choice of (m,n) with one even and one odd will lead to total reflection. Fig. 4 shows three total reflection cases created with $(m,n)=(1,2)$, $(m,n)=(1,4)$, and $(m,n)=(2,3)$.

Similarly, total transmission with right isosceles triangular defect can be obtained by choosing (m,n) either both even, or both odd, or $m=n$. In Fig. 5, we showed three cases obtained with $m=n=2$, $(m,n)=(1,3)$, and $(m,n)=(2,4)$, respectively.

Finally, in Fig. 6 and Fig. 7, we show that total reflection and transmission can be obtained for the 30-60-90 degrees triangular defect by choosing (m,n) properly, since the corresponding eigenfunction is $\phi^a_{n,m}$ given before for the equilateral triangle case.

https://doi.org/10.4208/aamm.2014.m659 Published online by Cambridge University Press

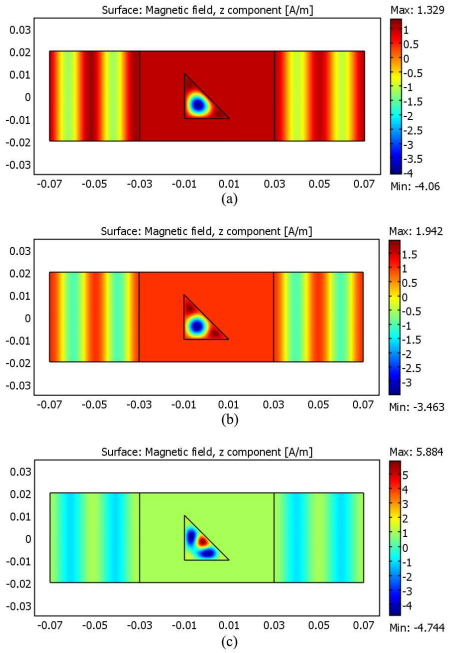


Figure 5: The H_z field for the equilateral triangular defect with $m=n=2$ (a), $m=1$, $n=3$ (b), and $m=2$, $n=4$ (c).

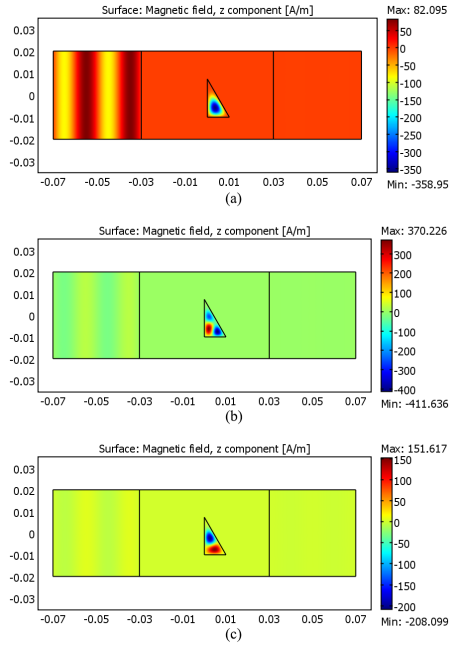


Figure 6: The H_z field for the 30-60-90 triangular defect with $m=n=2$ (a), $m=n=3$ (b), $m=2,n=4$ (c).

https://doi.org/10.4208/aamm.2014.m659 Published online by Cambridge University Press

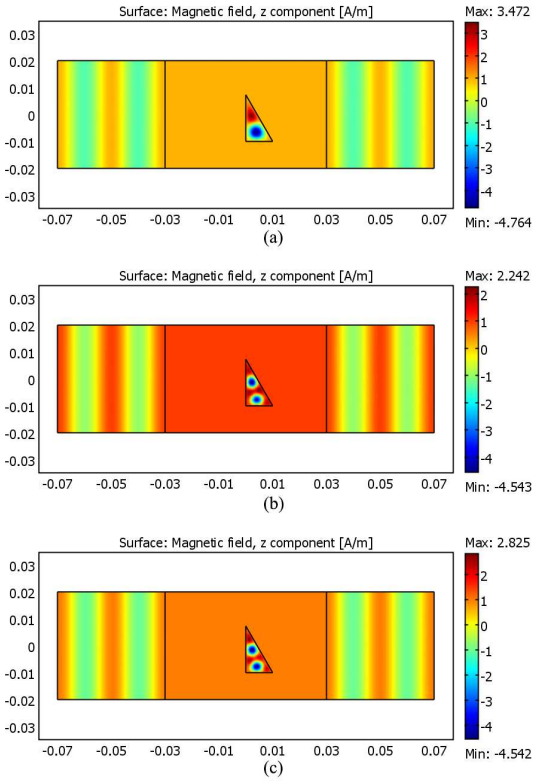


Figure 7: The H_z field for the 30-60-90 triangular defect with $m=1$, $n=2$ (a), $m=2$, $n=3$ (b), $m=1$, $n=3$ (c).

3 Conclusions

In conclusion, we have demonstrated how to achieve total reflection and total transmission of an EM wave for embedded triangular dielectric defects in the zero index metamaterial. Extensive numerical simulations confirm our theoretical analysis. Our work provides more flexibility in blocking wave or concealing objects by embedding defects of different triangular shapes in ZIMs. In the future, we will extend the current work to time-domain by solving the time-domain Maxwell's equations [12,28] so that we can see clearly how total reflection and total transmission are achieved as the wave propagates across different regions.

Acknowledgments

Prof. Yunqing Huang is partially supported by NSFC Key Project 91430213, IRT1179 of PCSIRT and MOST 2010DFR00700. Prof. Jichun Li is Partially supported by NSFC project 11271310 and a grant from the Simons Foundation (#281296 to Jichun Li). Also, The authors would like to thank three anonymous referees for the helpful suggestions on

https://doi.org/10.4208/aamm.2014.m659 Published online by Cambridge University Press

improving the paper. J. Li likes to thank UNLV for granting his sabbatical leave in spring 2014 during which the work gets finished.

References

[1] R. W. Ziolkowski, *Propagation in and scattering from a matched metamaterial having a zero index of refraction,* Phys. Rev. E, 70 (2004), 046608.
[2] B. Edwards, A. Alú, M. E. Young, M. Silveirinha and N. Engheta, *Experimental verification of epsilon-near-zero metamaterial coupling and energy squeezing using a microwave waveguide,* Phys. Rev. Lett., 100 (2008), 033903.
[3] R. Liu, Q. Cheng, T. Hand, J. J. Mock, T. J. Cui, S. A. Cummer and D. R. Smith, *Experimental demonstration of electromagnetic tunneling through an epsilon-near-zero metamaterial at microwave frequencies,* Phys. Rev. Lett., 100 (2008), 023903.
[4] M. Silveirinha and N. Engheta, *Tunneling of electromagnetic energy through subwavelength channels and bends using ϵ-near-zero materials,* Phys. Rev. Lett., 97 (2006), 157403.
[5] H. F. Ma, J. H. Shi, W. X. Jiang and T. J. Cui, *Experimental realization of bending waveguide using anisotropic zero-index materials,* Appl. Phys. Lett., 101 (2012), 253513.
[6] J. Hao, W. Yan and M. Qiu, *Super-reflection and cloaking based on zero index metamaterial,* Appl. Phys. Lett., 96 (2010), 101109.
[7] X. Huang, Y. Lai, Z. H. Hang, H. Zheng and C. T. Chan, *Dirac cones induced by accidental degeneracy in photonic crystals and zero-refractive-index materials,* Nat. Mater., 10 (2011), 582.
[8] J. Luo, P. Xu, L. Gao, Y. Lai and H. Chen, *Manipulate the transmissions using index-near-zero or epsilon-near-zero metamaterials with coated defects,* Plasmonics, 7 (2012), 353.
[9] V. C. Nguyen, L. Chen and K. Halterman, *Total transmission and total reflection by zero index metamaterials with defects,* Phys. Rev. Lett., 105 (2010), 233908.
[10] Y. Xu and H. Chen, *Total reflection and transmission by epsilon-near-zero metamaterials with defects,* Appl. Phys. Lett., 98 (2011), 113501.
[11] Y. Wu and J. Li, *Total reflection and cloaking by zero index metamaterials loaded with rectangular dielectric defects,* Appl. Phys. Lett., 102 (2013), 183105.
[12] J. Li and Y. Huang, Time-Domain Finite Element Methods for Maxwell's Equations in Metamaterials, Springer Series in Computational Mathematics, Vol. 43, Springer, January 2013.
[13] B. J. McCartin, *Eigenstructure of the equilateral triangle, Part I: The Dirichlet problem,* SIAM Rev., 45(2) (2003), pp. 267–287.
[14] A. Damle and G. C. Peterson, *Understanding the eigenstructure of various triangles,* SIAM Undergraduate Research Online, 3(1) (2010), pp. 187–208.
[15] A. Greenleaf, M. Lassas and G. Uhlmann, *On nonuniqueness for Calderón's inverse problem,* Math. Res. Lett., 10 (2003), pp. 685–693.
[16] G. W. Milton and N.-A. P. Nicorovici, *On the cloaking effects associated with anomalous localized resonance,* Proc. R. Soc. Lond. Ser. A, 462 (2006), pp. 3027–3059.
[17] J. B. Pendry, D. Schurig and D. R. Smith, *Controlling electromagnetic fields,* Science, 312 (2006), pp. 1780–1782.
[18] U. Leonhardt, *Optical conformal mapping,* Science, 312 (2006), pp. 1777–1780.
[19] R. Kohn, H. Shen, M. Vogelius and M. Weinstein, *Cloaking via change of variables in electrical impendance tomography,* Inverse Problems, 24 (2008), 015016.

https://doi.org/10.4208/aamm.2014.m659 Published online by Cambridge University Press

[20] F. Guevara Vasquez, G. W. Milton and D. Onofrei, *Broadband exterior cloaking,* Opt. Express, 17(2009), pp. 14800–14805.
[21] A. Greenleaf, Y. Kurylev, M. Lassas and G. Uhlmann, *Cloaking devices, electromagnetics wormholes and transformation optics,* SIAM Rev., 51 (2009), pp. 3–33.
[22] H. Ammari, H. Kang, H. Lee, M. Lim and S. Yu, *Enhancement of near cloaking for the full Maxwell equations,* SIAM J. Appl. Math., 73 (2009), pp. 2055–2076.
[23] J. Li and Y. Huang, *Mathematical simulation of cloaking metamaterial structures,* Adv. Appl. Math. Mech., 4(1) (2012), pp. 93–101.
[24] J. Li, Y. Huang and W. Yang, *Developing a time-domain finite-element method for modeling of electromagnetic cylindrical cloaks,* J. Comput. Phys., 231 (2012), pp. 2880–2891.
[25] G. Bao and H. Liu, *Nearly cloaking the electromagnetic fields,* SIAM J. Appl. Math., 74(3) (2014), pp. 724–742.
[26] G. Bao, H. Liu and J. Zou, *Nearly cloaking the full Maxwell equations: cloaking active contents with general conducting layers,* J. Math. Pure Appl., 101 (2014), pp. 716–733.
[27] J. Li, Y. Huang, W. Yang and A. Wood, *Mathematical analysis and time domain finite element simulation of carpet cloak,* SIAM J. Appl. Math., 74(4) (2014), pp. 1136–1151.
[28] Y. Huang, J. Li and Y. Lin, *Finite element analysis of Maxwell's equations in dispersive lossy bi-isotropic media,* Adv. Appl. Math. Mech., 5(4) (2013), pp. 494–509.

https://doi.org/10.4208/aamm.2014.m659 Published online by Cambridge University Press